SCIENTIFIC REPORTS

OPEN

SUBJECT AREAS:
NANOPARTICLES
SOLID-STATE CHEMISTRY
MATERIALS CHEMISTRY
ELECTROCATALYSIS

Received
3 April 2013

Accepted
8 July 2013

Published
23 July 2013

Correspondence and requests for materials should be addressed to Z.-G.Z. (zgzhao2011@sinano.ac.cn); H.L. (lvhong@tongji.edu.cn) or Q.-W.L. (qwli2007@sinano.ac.cn)

In-Situ Formation of Cobalt-Phosphate Oxygen-Evolving Complex-Anchored Reduced Graphene Oxide Nanosheets for Oxygen Reduction Reaction

Zhi-Gang Zhao[1], Jing Zhang[1], Yinyin Yuan[1], Hong Lv[2], Yuyu Tian[1], Dan Wu[1] & Qing-Wen Li[1]

[1]Suzhou Institute of Nano-Tech and Nano-Bionics, Ruoshui Road 398, Suzhou 215123, China, [2]Clean Energy Automotive Engineering Center, School of Automotive Studies, Tongji University, Shanghai 201804, China.

Oxygen conversion process between O_2 and H_2O by means of electrochemistry or photochemistry has lately received a great deal of attention. Cobalt-phosphate (Co-Pi) catalyst is a new type of cost-effective artificial oxygen-evolving complex (OEC) with amorphous features during photosynthesis. However, can such Co-Pi OEC also act as oxygen reduction reaction (ORR) catalyst in electrochemical processes? The question remains unanswered. Here for the first time we demonstrate that Co-Pi OEC does be rather active for the ORR. Particularly, Co-Pi OEC anchoring on reduced graphite oxide (rGO) nanosheet is shown to possess dramatically improved electrocatalytic activities. Differing from the generally accepted role of rGO as an "electron reservoir", we suggest that rGO serves as "peroxide cleaner" in enhancing the electrocatalytic behaviors. The present study may bridge the gap between photochemistry and electrochemistry towards oxygen conversion.

One great challenge in our modern society is unquestionably energy conversion, in which conversion between O_2 and H_2O plays an important role[1–4]. The oxygen evolution reaction (OER) from H_2O to O_2 generates molecular oxygen, converting solar energy or electric energy to chemical energy, while the oxygen reduction reaction (ORR) from O_2 to H_2O in the opposite direction is crucial in converting chemical energy into electric energy. The conversion between O_2 and H_2O can be realized mainly via two routes: photochemical and electrochemical process. It is highly challenging but desirable to develop efficient bifunctional catalysts on which both electrochemical and photochemical oxygen conversion occurs since such bifunctional catalysts could be readily used in optoelectronic integrated energy conversion devices.

Oxygen-evolving complex (OEC), well known as water splitting complex, is a water-oxidizing catalyst breaking down H_2O and creating molecular oxygen (O_2) during the light reactions of photosynthesis in plants, algae and cyanobacteria[1,5,6]. In nature, the OEC has a metalloenzyme core containing both manganese and calcium with the empirical formula of $Mn_4Ca_1O_xCl_{1-2}(HCO_3)_y$[5]. Biomimetically, Nocera and coworkers recently developed a new type of artificial OEC with amorphous features composed of cobalt, oxygen, and phosphate, normally called as cobalt-phosphate (Co-Pi) OEC, which is formed through the oxidation of Co^{2+} to Co^{3+} ion in aqueous neutral phosphate medium containing Co^{2+} ions[7–12]. Although the exact structure of the Co-Pi OEC has been hard to determine experimentally, this OEC offers many attractive features for artificial photosynthesis such as simple synthesis procedure, low cost, mild operation condition, and self-repair mechanism[7]. The catalytic mechanism of the Co-Pi OEC involves O_2/H_2O cycles of water oxidation at cobalt centers, while the phosphate is responsible for the self-healing of Co-Pi OEC[8,11]. Currently, Co-Pi OEC is becoming increasingly important for photochemical oxygen conversion process.

However, Co-Pi OEC has seldom been employed for electrochemical oxygen conversion process until now. The similarities between electrochemical and photochemical processes drive us to exploit the possibility of using such Co-Pi OEC catalyst in oxygen conversion via electrochemical processes. Furthermore, cobalt-based materials harbour conspicuous electrochemical properties and possess advantages of high abundance, low cost, and environmentally benign[13], which provides promises for Co-Pi OEC also working as efficient electrocatalysts for the ORR. To date, some cobalt compounds have been proved to show some ORR electrocatalytic activities[14,15], which are often very low though. Recent advances show that a much higher ORR activity can be obtained through

combining with support of reduced graphite oxide (rGO) nanosheet. A series of hybrid materials for use as ORR catalysts with high activity and stability has been synthesized, such as Co_3O_4/rGO[14,15], $Co_{1-x}S$/rGO[16], $MnCo_2O_3$/rGO[17], FePt/rGO[18], MoS_2/rGO[19]. The enhanced catalytic performance was attributed to the synergetic effect in catalyst/rGO support systems, where the interface boundary sites of catalyst/rGO support were believed to greatly influence the enhancement effect. Therefore, in our case, it is highly interesting to hybridize rGO nanosheet with Co-Pi to afford more efficient ORR catalysts (Figure 1). To this end, strong coupling of supported electrocatalysts to rGO is greatly needed[14–19], which can be obtained by in-situ electrodeposition technique. Herein, we report for the first time the in-situ synthesis of Co-Pi on rGO for ORR using an electrodeposition technique. The resulting Co-Pi anchored rGO nanosheet (rGO-Co-Pi) was found to be rather active for ORR in KOH solutions. The hybridization of rGO nanosheet leads to a clear enhancement in the electron-transfer kinetics of oxygen reduction especially at higher rotation rates. Furthermore, the present study provides us with a mechanism message on the novel role of rGO nanosheet for ORR as "peroxide cleaner", which is quite different from the widely accepted role as "electron reservoir".

Results

Co-Pi nanoparticles were electrodeposited potentiostatically onto the rGO nanosheet surface by placing a rGO nanosheet modified glassy carbon electrode into a 0.1 M potassium phosphate solution (pH 7) containing 0.5 mM $CoCl_2$ in a three-electrode electrochemical cell[7–12]. For a comparison, sole electrodeposited Co-Pi layers were also synthesized on glassy carbon electrode in the same way in the absence of rGO. The resulting rGO-Co-Pi product was characterized by scanning electron microscopy (SEM), energy dispersive spectroscopy (EDX) and X-ray photoelectron spectroscopy (XPS). Figures 2a and 2b show the representative SEM images of the as-prepared rGO-Co-Pi, disclosing that the rGO nanosheets are uniformly decorated with the electrochemically deposited Co-Pi nanoparticles with featureless shapes to form a spotted fabric-like structure. The observed sizes of Co-Pi nanoparticles in Figures 2a, b are about 50–200 nm. Using EDX analysis, it was found that C from rGO nanosheet, and Co, P, O, K from Co-Pi OEC are the principal elemental components (Figure 2c). The Co-Pi composition is consistent with the results obtained by other investigations[7,8]. The recorded Cl signal could be due to the residual $CoCl_2$ physically bound to the surface of rGO nanosheet or Co-Pi. XPS was conducted to examine the compositions and element chemical states, and the full-scale spectrum is shown in Figure 2d, confirming the formation of rGO-Co-Pi hybrid. As illustrated in the high-resolution Co 2p and P 2p spectra, two peaks located at about 780.4 and 795.9 eV can be assigned to Co^{2+} or Co^{3+} bound to oxygen (Figure 2e), and the P 2p peak at 132.7 eV is consistent with phosphate (Figure 2f). The aforementioned characterizations point to that the resulted material contains similar Co-Pi structures found in previous studies[7–12].

The ORR catalytic activities of Co-Pi and rGO-Co-Pi were first evaluated through conventional three-electrode cyclic voltammetry (CV) in O_2 or N_2 saturated 0.1 M KOH aqueous solutions. Both Co-Pi and rGO-Co-Pi electrode materials show a substantial reduction process in the presence of O_2, whereas no obvious response was observed under N_2 (Figures 3a and b). The well-defined characteristic ORR peak for Co-Pi layer is centered at −0.39 V, while it shifts positively to around −0.21 V under the same condition upon hybridization with rGO nanosheets, indicating an easier ORR process on rGO-Co-Pi.

To further investigate the ORR performances, we carried out the linear sweep voltammetric (LSV) measurements on a rotating disk electrode (RDE) with sole Co-Pi layer and rGO-Co-Pi in an O_2-saturated 0.1 M KOH electrolyte solution (Figures 3c and 3d). At both lower rotating rate of 200 rpm and higher rotating rate of 1200 rpm, the onset potential for rGO-Co-Pi (ca. −0.13 V) is more positive that that for Co-Pi layer, which is at about −0.27 V, suggesting that the coupling with rGO nanosheets indeed leads to a significant enhancement in the catalysis for the ORR. The diffusion current density of rGO-Co-Pi is also notably stronger than that of sole Co-Pi layer over a large potential range (−0.2–−0.8 V) with difference being widened at a higher rotating rate. Typical CV curves of the electrodes at other rotation rates also confirmed this tendency (vide post). Thus, it is clear that Co-Pi OEC can also work as electrocatalyst for ORR, with improved behaviors through forming hybrid with rGO nanosheets. Furthermore, the degree in enhancement of ORR activity is dependent on the rotational speed, which gives a clue to understanding the role of rGO nanosheet in ORR.

Discussion

To gain further insight into the ORR behaviors of Co-Pi and rGO-Co-Pi, the corresponding ORR kinetics were investigated, recording LSV curves at various rotation rates (Figures 4a and 4b). Compared with Co-Pi, rGO-Go-Pi gives more defined diffusion-controlled LSV waves. With increase in rotation rate, the limiting current density

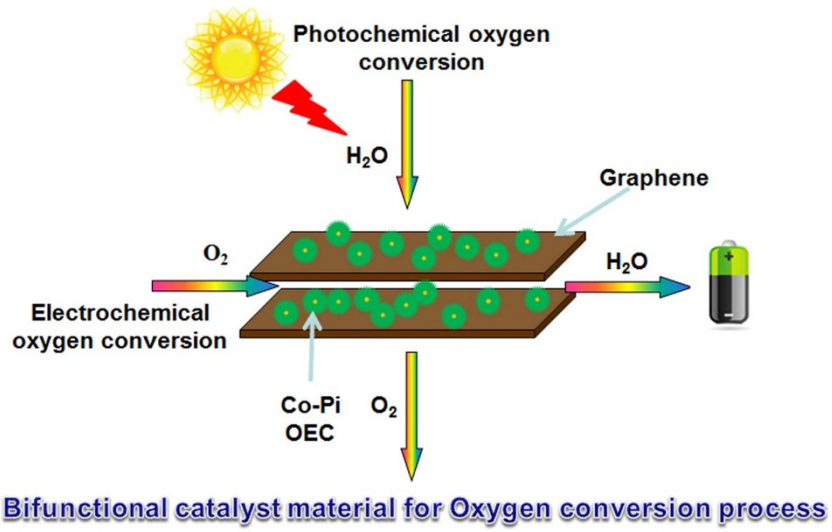

Figure 1 | Roles of rGO-Co-Pi in oxygen conversion. Schematic illustration of Co-Pi OEC materials anchoring on rGO nanosheet working as a novel class of bifunctional catalyst material for both electrochemical and photochemical oxygen conversion.

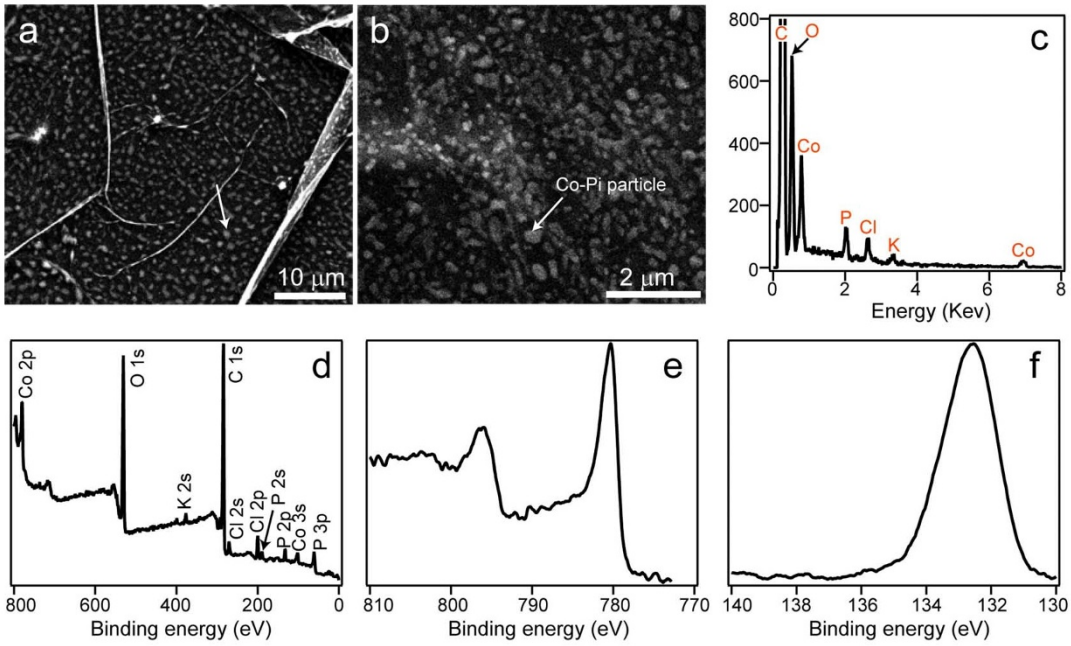

Figure 2 | **Characterization of rGO-Co-Pi.** SEM images of spotted fabric-like rGO-Co-Pi obtained by direct electrodeposition technique at (a) low and (b) high magnification showing the uniform distribution of Co-Pi particles on rGO nanosheet; (c) EDX spectrum showing the elemental composition of the resultant rGO-Co-Pi; (d) XPS survey spectrum, (e) high resolution Co 2p and (d) P 2p spectrum for rGO-Co-Pi. Signals arising from rGO nanosheet and Co-Pi were mainly detected. The Cl signals are due to trace residual $CoCl_2$ on the surface.

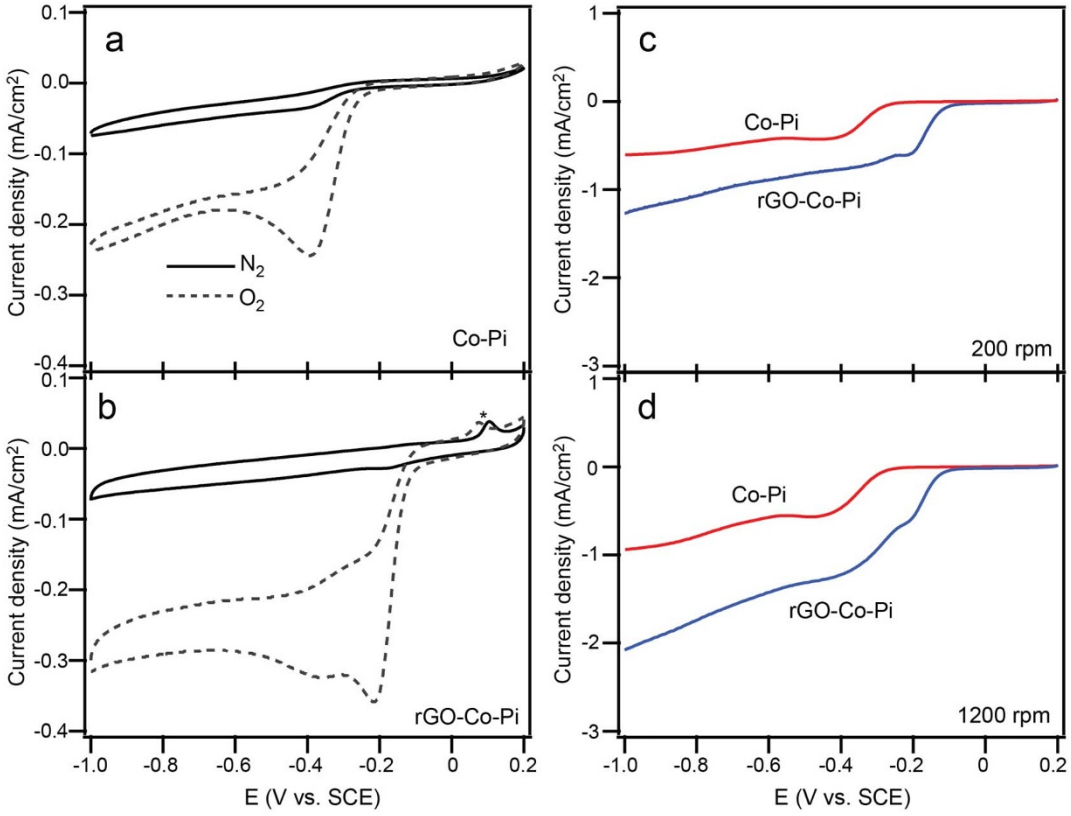

Figure 3 | **Electrochemical performance of Co-Pi and rGO-Co-Pi.** CV curves of ORR on Co-Pi (a) and rGO-Co-Pi (b) in N_2- (solid) and O_2-saturated (dotted) 0.1 M KOH solutions at a scan rate of 20 mVs^{-1}. Cathodic peaks occur only in O_2-saturated solutions, and the peak position for rGO-Co-Pi hybrid is more positive, suggesting that rGO-Co-Pi more favors ORR. A weak peak marked with asterisk appears in the curve for rGO-Co-Pi, which is supposed to originate from rGO. LSV curves at rotation speeds of 200 rpm (c) and 1200 rpm (d) for oxygen reduction in O_2-saturated 0.1 M KOH solutions. rGO-Co-Pi hybrid exhibits more positive onset potential and higher current density. Meanwhile, the difference in current density between the two electrodes is widened at a higher rotation speed.

also increases. Furthermore, the limiting current density of ORR on rGO-Co-Pi electrode is always higher than that on Co-Pi electrode at each rotation rate, suggesting better ORR activity on rGO-Co-Pi electrode. The transferred electron numbers per O_2 molecule involved in ORR at both Co-Pi and rGO-Co-Pi electrodes can be determined by Koutecky-Levich (K–L) equation as given below[15–19]:

$$1/j = 1/jk + 1/B\omega^{0.5} \quad (1)$$

Where j is the measured current density, j_k is the kinetic current, ω is the electrode rotating rate. B could be determined from the slope of the K–L plots in Figures 4c and 4d based on the Levich equation:

$$B = 0.2nFC_0D_0^{2/3}\eta^{-1/6} \quad (2)$$

Where n represents the transferred electron numbers per O_2 molecule, F is the Faraday constant (F = 96485 C mol^{-1}), C_o is the concentration of O_2 in the electrolyte (Co = 1.2 × 10^{-6} mol cm^{-3}), D_0 is the diffusion coefficient of O_2 (D_0 = 1.9 × 10^{-5} cm^2 s^{-1}), and η is viscosity of electrolyte (η = 0.01 cm^2 s^{-1}). Using B factor, the numbers of electrons transferred associated with ORR for both Co-Pi and rGO-Co-Pi were calculated. As shown in Figure 4e,

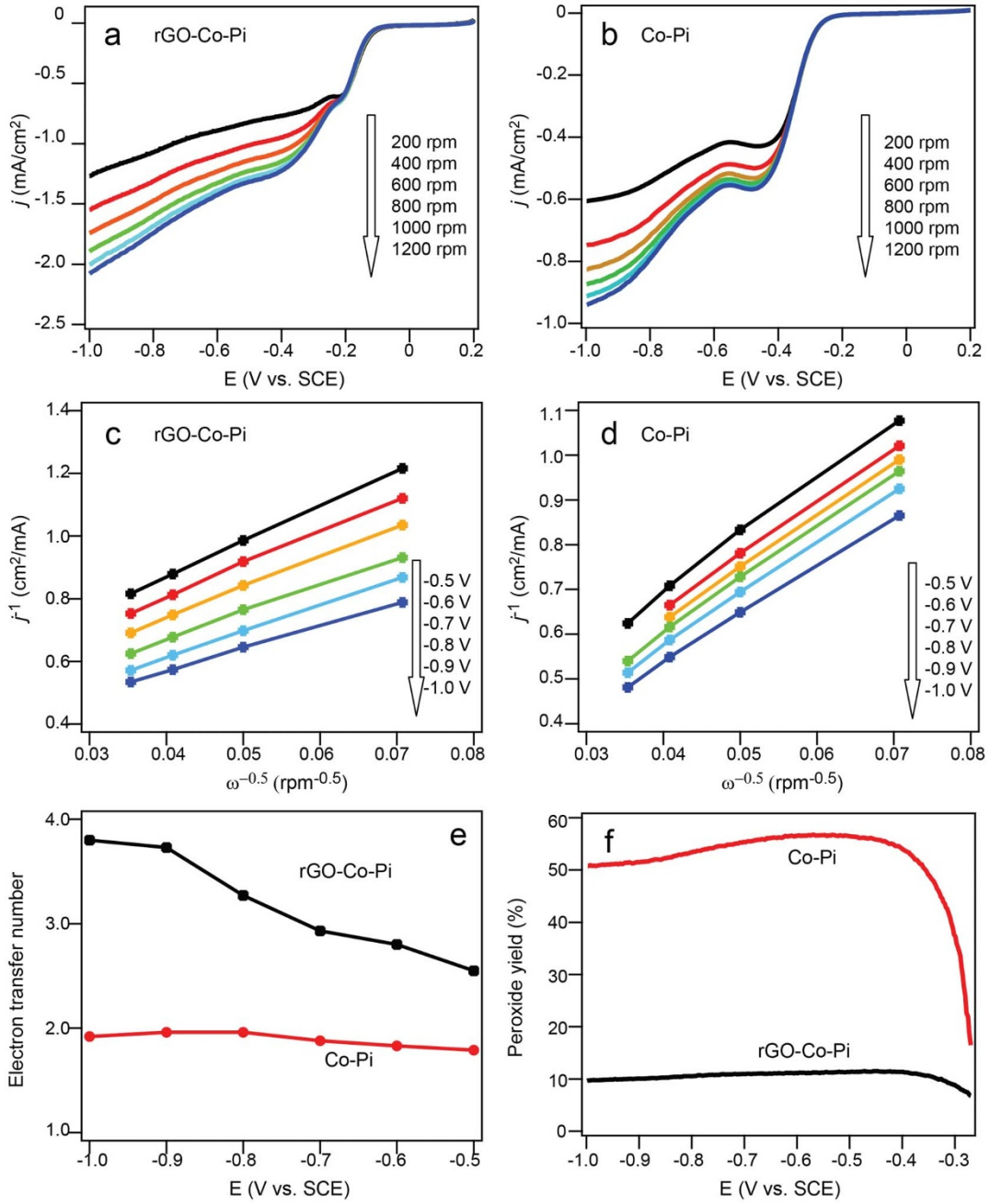

Figure 4 | Analysis of oxygen reduction on pure Co-Pi and rGO-Co-Pi. LSV curves at various different rotation rates for (a) rGO-Co-Pi showing well-defined diffusion-controlled wave in comparison with ill-defined wave for sole Co-Pi (b). The current density for rGO-Co-Pi is obviously higher than that for Co-Pi. K-L plots on (c) G-Co-Pi and (d) pure Co-Pi layer having good linear relationship; (e) the dependence of the electron transfer number on the potential for both G-Co-Pi (black line) and sole Co-Pi layer (red line) suggesting that four-electron process also joins the ORR after hybridization with rGO; (f) Peroxide yield of G-Co-Pi (black line) and sole Co-Pi layer (red line) at various potentials in an O_2-saturated 0.1 M KOH solution (The Pt ring electrode was polarized at 0 V for oxidizing H_2O_2 intermediate). The peroxide intermediate is much more depressed in rGO-Co-Pi, indicating that rGO efficiently improves the ORR behaviors of Co-Pi electrode.

the electron transfer number was found to be dependent on the potentials. The electron transfer numbers for Co-Pi layer from −0.5 V to −1.0 V were calculated to be between 1.79–1.92, thereby indicating that the ORR is dominated by a two-electron process under these voltages. However, the electron transfer numbers for rGO-Co-Pi are higher at 2.55–3.8 over the potential range, suggesting an oxygen reduction process with combined two-electron and four-electron reaction pathways. The higher electron transfer numbers indicate a more efficient ORR process over rGO-Co-Pi. In addition, the amount of the ORR reaction intermediate, peroxide, was determined using the current potential curves recorded at the disk and the ring at 1200 rpm in O_2 saturated solution based on the equation 3: (Figure 4f).

$$H_2O_2(\%) = 200 \times I_r/((N \times I_d) + I_r) \quad (3)$$

Here I_d and I_r is the disk current and ring current, respectively, and N is the collection efficiency (0.37) of the ring electrode. The calculated peroxide yield is about 10% for rGO-Co-Pi hybrid over the range from −0.4 V to −1.0 V vs SCE, while it is beyond 50% for sole Co-Pi layer. These results further indicates that the rGO-Co-Pi is more favorable for ORR than the sole Co-Pi layer.

Very recently, rGO has been used as an effective support for certain nanoparticles such as FePt, Fe_3O_4 and Co_3O_4 to improve ORR catalytic activity and stability[14–19]. It has been reported that metal oxide/metal or rGO alone has little ORR catalytic activity, while the resulting strongly coupled hybrid exhibits much increased ORR activity than free metal oxide/metal, free rGO and even their physical mixture. In previous reports, the improved behavior was attributed to rGO working as an "electron reservoir" to trap electrons from electrocatalysts, and therefore charge transfer across the metal oxide/metal-rGO interface was supposed to be the main reason for the synergistic enhancement effect[15]. Based on our experimental results, we propose a different electrocatalytic mechanism where the role of rGO acts as a "peroxide cleaner" in our system. The average electron transfer number, 1.79–1.92 and 2.55–3.8 for Co-Pi and rGO-Co-Pi, respectively, suggests that 2-electron reduction pathway plays an important role in the reduction of oxygen for both the two materials. In this case, peroxide is the main reaction intermediate for the ORR, and its further reaction is an essential factor for the complete reduction of oxygen. When the rotation rate is low, the reaction rate and concentration of generated peroxide is low, and correspondingly rGO has a relatively less effect on ORR activities. The increase in rotation rate may result in speed up of the reaction and accumulation of the intermediate peroxide, and afterwards peroxide might be adsorbed to the surface of electrocatalysts, which probably blocks the active sites for further dissociating adsorption of oxygen. Therefore the removal speed of peroxide is a rate-limiting factor for the ORR. If the rGO could effectively catalyze the reduction of peroxide as a "peroxide cleaner", the ORR activity would be largely enhanced[20,21]. A controlled experiment was performed to confirm the above inference on the role of rGO. Figure 5 shows CVs for rGO nanosheets in N_2-saturated 0.1 M KOH (solid line) and 0.1 M KOH + 0.2 M H_2O_2 solution (dotted line). A broad, relatively large reduction peak was observed at about −0.32 V on the cathodic scan in KOH + H_2O_2 solution corresponding to the reduction of peroxide catalyzed by rGO nanosheets, while no such peak appears in KOH solution, which corroborates that the rGO nanosheets does play a role as "peroxide cleaner".

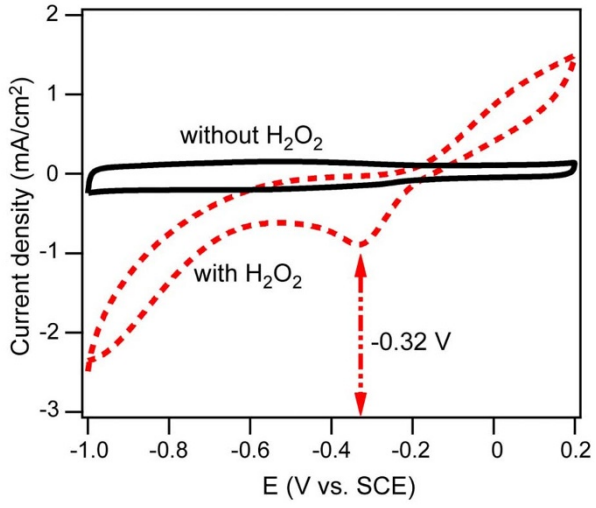

Figure 5 | A controlled experiment confirming the role of rGO nanosheet as "peroxide cleaner". CVs on rGO nanosheet modified glassy carbon electrode in N_2-saturated 0.1 M KOH solutions (solid line) and in N_2-saturated 0.1 M KOH + 0.2 M H_2O_2 (dotted line) with peak occurrence in solutions containing H_2O_2 at ca. −0.32 V corresponding to reduction of peroxide.

In summary, we have described the first design of rGO-Co-Pi as efficient electrocatalysts for the ORR. As Co-Pi material is also an excellent oxygen-evolving complex during photosynthesis, this novel material can undergo two pairs of oxygen conversion process (electrochemical and photochemical) as a bifunctional catalyst. Compared to Co-Pi OEC, the rGO-Co-Pi exhibits much enhanced electrocatalytic activity for the ORR in O_2-saturated KOH solution. The ORR activity enhancement induced by the addition of rGO shows dependence on the rotational speed. Possible mechanisms are proposed for the ORR reaction of rGO-Co-Pi hybrid, in which rGO nanosheets could play a role as "peroxide cleaner" to speed up the ORR rates. This work demonstrates that the rGO-Co-Pi may serve as a novel class of bifunctional catalyst material that is applicable to future optoelectronic integrated energy conversion devices. The present study may also bridge the gap between photochemistry and electrochemistry towards oxygen conversion.

Methods

Synthesis of G-Co-Pi. Co-Pi OEC nanoparticles were electrodeposited potentiostatically onto the reduced graphene oxide (rGO) surface via chronoamperometry technique by placing an rGO nanosheet-modified glassy carbon electrode under static conditions reported by Nocera et al[7,8]. A three-electrode cell was used with an rGO nanosheet-modified glassy carbon electrode as the working electrode. An SCE electrode and Pt foil were used as reference and counter electrode, respectively. 1.1 V was applied in a solution of 0.5 mM $CoCl_2$ in 0.1 M KH_2PO_4 at pH 7. The amount of Co-Pi OEC nanoparticles deposited can be controlled by the deposition time, which ranged between 200 and 500 s. Current densities were typically about 0.05 to 1.5 $mAcm^{-2}$ during deposition.

Characterization. Field emission scanning electron microscopy (FE-SEM) analysis was performed on a FEI Quanta 400 FEG field emission scanning electron microscope. Energy-dispersive X-ray spectra (EDS) were collected from an attached Apollo 40 SDD energy-dispersive spectrometer fixed on a FEI Quanta 400 FEG field emission scanning electron microscope. X-ray photoelectron spectra (XPS) were acquired on an X-ray photoelectron spectroscopy (Thermo Escalab 250, a monochromatic Al Kα X-ray source). The binding energies obtained were corrected for specimen charging by referencing C 1 s to 284.44 eV. Electrochemical measurements were carried out on an electrochemical workstation (Autolab PDSTAT 302N Auto 84082) using a conventional three-electrode test cell. A platinum wire was used as counter-electrode and saturated calomel electrode (SCE) as reference electrode. The geometric area of the working electrode is 0.2475 cm^2. The Pt ring electrode was polarized at 0.50 V for oxidizing H_2O_2 intermediate.

1. Nocera, D. G. The Artificial Leaf. *Acc. Chem. Res.* **45**, 767–776 (2012).
2. Nocera, D. G. Chemistry of personalized solar energy. *Inorg.Chem.* **48**, 10001–10017 (2009).
3. Stephens, I. E. L., Bondarenko, A. S., Gronbjerg, U., Rossmeisl, J. & Chorkendorff, I. Understanding the electrocatalysis of oxygen reduction on platinum and its alloys. *Energy. Environ. Sci.* **5**, 6744–6762 (2012).
4. Zhao, Y. *et al.* A Versatile, Ultralight, Nitrogen-Doped Graphene Framework. *Angew. Chem. Int. Ed.* **51**, 11371–11375 (2012).
5. King, R. B. Encyclopedia of inorganic chemistry. Wiley InterScience (2005).
6. Najafpour, M. M. & Govindjee. Oxygen evolving complex in Photosystem II: Better than excellent. *Dalton Trans.* **40**, 9076–9084 (2011).

7. Kanan, M. W. & Nocera, D. G. In Situ Formation of an Oxygen-Evolving Catalyst in Neutral Water Containing Phosphate and Co^{2+}. *Science* **321**, 1072–1075 (2008).
8. Reece, S. Y. *et al.* Wireless Solar Water Splitting Using Silicon-Based Semiconductors and Earth-Abundant Catalysts. *Science* **334**, 645–648 (2011).
9. Zhong, D. K., Cornuz, M., Sivula, K., Gratzel, M. & Gamelin, D. R. Photo-assisted electrodeposition of cobalt-phosphate (Co-Pi) catalyst on hematite photoanodes for solar water oxidation. *Energy. Environ. Sci.* **4**, 1759–1764 (2011).
10. Seabold, J. A. & Choi, K. S. Effect of a Cobalt-Based Oxygen Evolution Catalyst on the Stability and the Selectivity of Photo-Oxidation Reactions of a WO_3 Photoanode. *Chem. Mater.* **23**, 1105–1112 (2011).
11. Steinmiller, E. M. P. & Choi, K. S. Photochemical deposition of cobalt-based oxygen evolving catalyst on a semiconductor photoanode for solar oxygen production. *P. Natl. Acad. Sci. USA* **49**, 20633–20636 (2009).
12. Lutterman, D. A., Surendranath, Y. & Nocera, D. G. A self-healing oxygen-evolving catalyst. *J. Am. Chem. Soc.* **131**, 3838–3839 (2009).
13. Tang, C. W., Wang, C. B. & Chien, S. H. Characterization of cobalt oxides studied by FT-IR, Raman, TPR and TG-MS. *Thermochimica Acta* **473**, 68–73 (2008).
14. Liang, Y. Y., Li, Y. G., Wang, H. L., Zhou, J. G. & Dai, H. J. Co_3O_4 nanocrystals on graphene as a synergistic catalyst for oxygen reduction reaction. *Nat. Mater.* **10**, 780–786 (2011).
15. Guo, S. J., Zhang, S., Wu, L. H. & Sun, S. H. Co/CoO Nanoparticles Assembled on Graphene for Electrochemical Reduction of Oxygen. *Angew. Chem. Int. Ed.* **51**, 11770–11773 (2012).
16. Wang, H. L., Liang, Y. Y., Li, Y. G. & Dai, H. J. $Co_{1-x}S$–Graphene Hybrid: A High-Performance Metal Chalcogenide Electrocatalyst for Oxygen Reduction. *Angew. Chem. Int. Ed.* **50**, 10969–10972 (2011).
17. Liang, Y. *et al.* Covalent Hybrid of Spinel Manganese Cobalt Oxide and Graphene as Advanced Oxygen Reduction Electrocatalysts. *J. Am. Chem. Soc.* **134**, 3517–3523 (2012).
18. Guo, S. J. & Sun, S. H. FePt Nanoparticles Assembled on Graphene as Enhanced Catalyst for Oxygen Reduction Reaction. *J. Am. Chem. Soc.* **134**, 2492–2495 (2012).
19. Li, Y. G. *et al.* MoS_2 Nanoparticles Grown on Graphene: An Advanced Catalyst for the Hydrogen Evolution Reaction. *J. Am. Chem. Soc.* **133**, 7296–7299 (2011).
20. Britto, P. J., Santhanam, S. V., Rubio, A., Alonso, J. A. & Ajayan, P. M. Improved Charge Transfer at Carbon Nanotube Electrodes. *Adv. Mater.* **11**, 154–157 (1999).
21. Xu, W. L., Zhou, X. C., Liu, C. P., Xing, W. & Lu, T. H. The real role of carbon in Pt/C catalysts for oxygen reduction reaction. *Electrochem. Commun* **9**, 1002–1006 (2007).

Acknowledgements

This work was supported by National Natural Science Foundation of China (51102274, 21273269), 973 project (No. 2011CB932600).

Author contributions

Z.G.Z. conceived the experiments, analyzed the results, and wrote the paper. Z.G.Z., J.Z., Y.Y.Y., H.L. and Y.Y.T. performed the experiments. D.W. and Q.W.L. helped with data analysis. All authors reviewed the paper.

Additional information

Supplementary information accompanies this paper at http://www.nature.com/scientificreports

Competing financial interests: The authors declare no competing financial interests.

How to cite this article: Zhao, Z.-G. *et al.* In-Situ Formation of Cobalt-Phosphate Oxygen-Evolving Complex-Anchored Reduced Graphene Oxide Nanosheets for Oxygen Reduction Reaction. *Sci. Rep.* **3**, 2263; DOI:10.1038/srep02263 (2013).